

## Composite Power Laws in Shock Fragmentation

Anders Meibom and Ivar Balslev

*Physics Department, Odense University, DK-5230 Odense M, Denmark*  
(Received 21 November 1995)

Inspired by the discovery of Oddershede *et al.* [Phys. Rev. Lett. **71**, 3107 (1993)] concerning the dimensionality dependence of mass distributions after shock fragmentation, we have performed further experiments using thick plates of dry clay. We observe mass distributions with composite power laws, i.e., different exponents for fragments larger and smaller than the plate thickness. This implies that the dominant exponent for any given fragment mass corresponds to the dimensionality of the original object on the length scale of the fragment considered. We study two profoundly different models, both of which agree qualitatively with the observed features. Thus the measured mass distribution tells little about the mechanisms of the fragmentation process.

PACS numbers: 46.30.Nz, 91.60.Ba

Shock fragmentation of solid objects has been studied extensively in the laboratory [1,2] and in geological and planetary systems [1,3]. The persistent pattern in the observations is a power law in the mass distribution. The exponent  $\beta$  in the differential mass distribution  $n(m) \propto m^{-\beta}$  is observed to be between 1.5 and 2 for a large variety of brittle materials. Essential new information on the dependence of this exponent on the shape of the fragmented body was reported by Oddershede, Dimon, and Bohr [4]. Their studies of fragmentations of cubes, plates, and rods show that  $\beta$  decreases markedly with decreasing dimensionality. They introduced a shape parameter  $d_m$  which for a box of dimension  $a \times b \times c$  is equal to  $1 + 2(ab + bc + ca)/(a^2 + b^2 + c^2)$ . The values for cubes, thin plates, and thin rods are 3, 2, and 1, respectively. The observed values of  $\beta$  for integer values of  $d_m$  are given in Table I. For objects of arbitrary forms the shape parameter may be noninteger. Oddershede, Dimon, and Bohr [4] find that the mass distribution is characterized by a simple power law on all length scales also for noninteger values of  $d_m$ .

In the present work we investigate in detail the fragmentation of thick plates giving values of  $d_m$  somewhat larger than 2. We concentrate our experiments on plates with thicknesses and applied impacts giving suitable fractions of fragments smaller than the plate thickness. Our results show that the universal scaling claimed in Ref. [4] does not hold for plates of dry clay and values of  $d_m$  in the range 2.1–2.3 (thick plates). We observe instead a composite power law with exponents for large and small fragments corresponding to those of two and three dimensions, respectively.

We report here the results of six fragmentation experiments similar to those of Ref. [4], i.e., we let solid objects

fall onto a hard floor. The material used was dry clay, and the height of the fall was 2.0 m. The fragments were collected and their mass distribution was recorded. We concentrated on objects in the form of square plates with thicknesses in the range 0.02–0.14 times the side length. Dimensions and masses of the clay plates are given in Table II.

The mass distribution of fragments can be described by the cumulative distribution  $F(m)$ , i.e., the number of observed fragments with mass larger than the mass  $m$ . Reference [4] uses the quantity  $N(m) = F(m)/m$ . We prefer to use  $F(m)$  in order to obtain clearer graphical representations. We show in Fig. 1 three distributions  $F(m)$  of fragments from plates with different thicknesses.  $F(m)$  is the integral of  $n(m)$  and so a double logarithmic plot of  $F(m)$  has the slope  $1 - \beta$ , if  $n(m)$  is proportional to  $m^{-\beta}$ .

Each distribution has a cutoff at large masses due to the finite size of the object and a cutoff at small masses due to poor sampling. In the following analysis we consider the region between these two cutoffs. It is clear from Fig. 1 that the power law is composite, i.e., the slopes  $\beta^+$  and  $\beta^-$  for large and small fragments, respectively, are different. We give in Table II the exponents found in the present work. The mass  $m_t$  separating the low-slope and the high-slope region was found. Table II gives values of  $m_t$  and of the ratio  $d_t/c$ , where  $d_t$  is the diameter of the sphere with mass  $m_t$  (using a mass density  $\rho$  of 2 g/cm<sup>3</sup>), and  $c$  is the plate thickness.

It is seen from Tables I and II that the exponents  $\beta^+$  for large fragments correspond to two dimensions and the exponents  $\beta^-$  for small fragments correspond to three dimensions. The fragment size separating the two- and the three-dimensional behavior is seen to be related to the

TABLE I. Values of the exponent  $\beta$  from experiments reported in Ref. [4].

$d_m =$ the dimensionality $D$	1	2	3
Experimental value of $\beta$ [4]	$1.0 \pm 0.1$	$1.2 \pm 0.1$	$1.55 \pm 0.1$

TABLE II. Results from fragmentation of 6 plates: masses, linear dimensions  $a$ ,  $b$ , and  $c$ , and exponents  $\beta^+$ ,  $\beta^-$  above and below a transitional mass  $m_t$ .  $d_t$  is the diameter of a sphere with mass  $m_t$  ( $\rho \approx 2 \text{ g/cm}^3$ ). The smallest fragments recorded in case of plates 7 and 8 were too large to allow a reliable determination of  $m_t$  and  $\beta^-$ .

Object	Mass (g)	$a$ (cm)	$b$ (cm)	$c$ (cm)	$m_t$ (g)	$d_t/c$	$\beta^-$	$\beta^+$
Plate 2	540.2	19.7	19.5	0.79	0.08	0.53	1.62	1.19
Plate 3	590.1	19.5	19.5	0.83	0.1	0.55	1.50	1.17
Plate 4	650.8	28.5	28.5	0.43	0.035	0.76	1.67	1.12
Plate 6	920.4	15.7	15.0	2.09	0.9	0.44	1.50	1.19
Plate 7	393.5	19.5	19.5	0.52	...	...	...	1.22
Plate 8	237.0	19.5	11.8	0.53	...	...	...	1.27

plate thickness. We find that the diameter  $d_t$  of a sphere with the mass  $m_t$  of the observed transition mass is 0.44–0.76 times the plate thickness (see Table II).

We conclude from these findings that *the exponent dominant in the formation of any given fragment is determined by the dimensionality of the original object on the length scale of the fragment considered*. In other words, the fragmentation mechanism depends on the local rather than the global properties of the original object.

After some of the fragmentations were formed, we reassembled the largest fragments, thereby establishing the coarsest part of the crack pattern. In Fig. 2(a) we show a crack pattern obtained by taking a photograph of the reassembled plate 6. This picture and pictures of other reassembled plates were subject to a wave analysis performed in the following two steps. First, we digitized the image of the crack patterns into a  $128 \times 128$  grey-tone bit map (resolution 8 bits per pixel). Then, we performed a two-dimensional discrete Fourier transformation of the

bit map. The transform of the picture in Fig. 2(a) is shown in Fig. 2(b). Note that the axes here are wave vector components ( $k_x, k_y$ ), and that the origin in wave vector space is in the middle of the picture. We note here the presence of pronounced spots in wave vector space [Fig. 2(b)]. This is an indication of standing waves prior to fragmentation. We assign the spots in wave vector space to modes responsible for the fracture. This indicates that it takes more than one vibrational cycle to build up the stress to the yield strength of the material.

We propose here two fundamentally different models giving the same qualitative behavior as measured, in particular, the composite power law for mixed dimensionality and the fact that exponent  $\beta$  increases with dimensionality. The first is a cascade type model and the second is based on a classification according to standing waves.

The first model is based on the assumption that the fragmentation process is a series of binary fissions. Here  $m$  and  $e$  are the mass and density of mechanical energy,

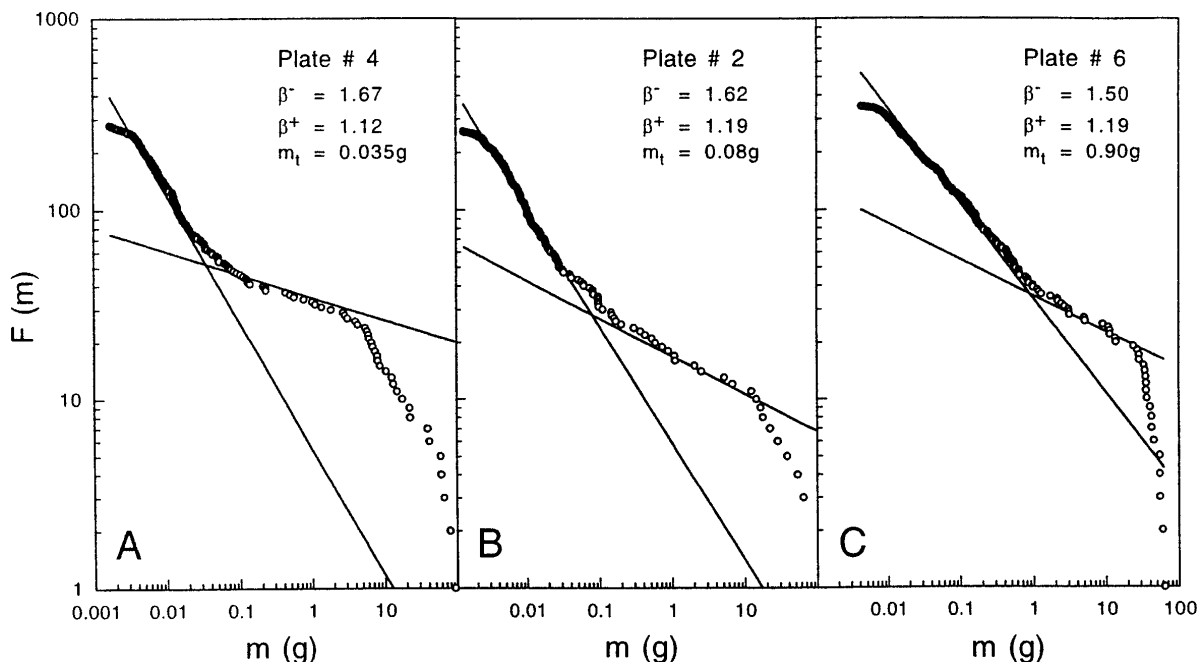


FIG. 1. Observed cumulative distributions  $F(m)$  defined as the number of fragments with mass larger than  $m$ . (a) Plate 4 (thickness 0.43 cm,  $m_t = 0.035 \text{ g}$ ); (b) plate 2 (thickness 0.79 cm,  $m_t = 0.08 \text{ g}$ ); (c) plate 6 (thickness 2.09 cm,  $m_t = 0.90 \text{ g}$ ). Note the correlation between the plate thickness and the transition mass  $m_t$  dividing the two power law regions.

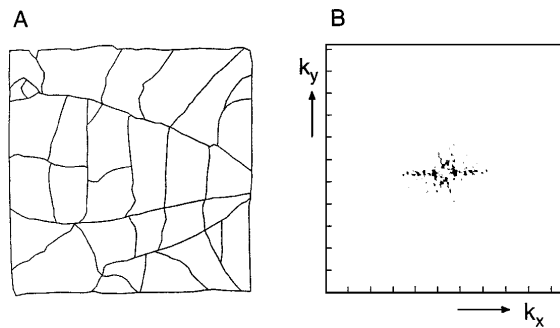


FIG. 2. (a) Crack pattern of plate 6. (b) Fourier transform of the pattern in (a). The black spots correspond to wave vector components with high absolute value.

respectively, of the object subject to fission. In three dimensions we assume the following in each fission: (i) The fragments have masses  $\alpha m$  and  $(1 - \alpha)m$  where  $\alpha$  is smaller than  $1/2$ . (ii) The loss of mechanical energy is  $s(\alpha m)^{2/3}$ , a quantity which is roughly proportional to the surface of the smallest fragment.  $s$  contains the formation energy per unit area during fracture, the mass density, and a geometrical factor. Then the average density of mechanical energy after the fission considered is reduced to a value given by  $e' = e - s(\alpha m)^{2/3}/m$ . Let  $\alpha_{\max}$  be the value of  $\alpha$  giving  $e' = 0$ . (iii)  $\alpha$  is chosen randomly between 0 and  $\alpha_{\max}$  or 0.5, whatever is smallest. (iv) Both fragments have the reduced energy density  $e'$ .

In the case of one and two dimensions, the above exponent  $2/3$  should be replaced by zero and  $1/2$ , respectively. We have performed Monte Carlo simulations along the above lines and find universal scaling with the following exponents:

$$\beta = \begin{cases} 1.0 & \text{for } D = 1, \\ 1.1 & \text{for } D = 2, \\ 1.15 & \text{for } D = 3, \end{cases} \quad (1)$$

where  $D$  is the dimensionality. Somewhat higher values of  $\beta$  are achieved if the two fragments contain equal residual energy rather than equal energy density.

The second model is inspired by the analysis of the coarse part of the crack pattern, and is based on the assumption that standing waves play an important role. The wave responsible for the formation of a fragment of mass  $m$  is assumed to have a wave length proportional to  $m^{1/D}$ , i.e., a wave vector  $k$  proportional to  $m^{-1/D}$ . The further assumptions are as follows: (i) The probability that any mode produces a fragment depends only on  $k$  and is assumed to be proportional to  $k^{-\gamma}$ . Here  $\gamma$  is a phenomenological parameter. (ii) The density of normal modes  $g(k)$  is proportional to  $k^{D-1}$  [5]. Then, the differential mass distribution  $n(m)$  has the following behavior:

$$\begin{aligned} n(m)dm &\propto k^{-\gamma} g(k) dk \propto m^{\gamma/D} m^{-(D-1)/D} \frac{dk}{dm} dm \\ &\propto m^{-2+\gamma/D} dm. \end{aligned} \quad (2)$$

Thus

$$\beta = 2 - \gamma/D. \quad (3)$$

If we assume  $\gamma$  to be about 1, independent of dimensionality, we get

$$\beta = \begin{cases} 1.0 & \text{for } D = 1, \\ 1.5 & \text{for } D = 2, \\ 1.66 & \text{for } D = 3. \end{cases} \quad (4)$$

Note that the temporal features in the fracture process are not specified in the standing-wave model. As the fracture process is probably best described as a series of events, the arguments about the density of modes should be applied to the individual events.

Comparing Eqs. (1) and (4) with Table I it is seen that the models are too crude to give the measured exponents in full detail; but both models exhibit universal scaling and give exponents which increase with dimensionality.

In summary, we have investigated the mass distribution after shock fragmentation of plates of dry clay. The most important experimental results are (1) there is a composite power law in the mass distribution of fragments from thick plates, and (2) the fragment size of the transition region scales with the plate thickness. These findings indicate that the exponent  $\beta$  is determined by local rather than global features of the original object. We have investigated two models giving universal scaling in case of "unmixed" dimensionalities. At the same time they account for the composite nature of the mass distribution from objects with "mixed" dimensionality.

We do not rank one model higher than the other. Instead we conclude from the theoretical part of the present work that the observed features can be explained by a large class of models, and so the mass distribution itself is a poor handle for exploring the detailed dynamics in the fragmentation process.

The authors are grateful for valuable discussions with H. Haack, P. Sibani, Mads Sckerl, and B. Ørsted.

- 
- [1] W. K. Hartmann, *Icarus* **10**, 201 (1969).
  - [2] A. Fujiwara, G. Kamimoto, and A. Tsukamoto, *Icarus* **31**, 277 (1977).
  - [3] A. Fujiwara, P. Ceroroni, D. Davis, E. Ryan, M. di Martinio, K. Holsapple, and K. Housen, in *Asteroids*, edited by R. P. Binzel, T. Gehrels, and M. S. Matthews (The University of Tucson Press, Tucson, 1989), Vol. II, p. 240.
  - [4] L. Oddershede, P. Dimon, and J. Bohr, *Phys. Rev. Lett.* **71**, 3107 (1993).
  - [5] C. Kittel, *Introduction to Solid State Physics* (Wiley and Sons, New York, 1986).